Journal of Insect Physiology 127 (2020) 104160

Contents lists available at ScienceDirect

Journal of Insect Physiology

journal homepage: www.elsevier.com/locate/jinsphys

Involvement of apolipoprotein D in desiccation tolerance and adult fecundity of *Acyrthosiphon pisum*

Jian-Wen Qiao [1], Yong-Liang Fan [1], Bing-Jin Wu, Dun Wang [*], Tong-Xian Liu [*]

State Key Laboratory of Crop Stress Biology for Arid Areas and Key Laboratory of Integrated Pest Management on Crops in Northwestern Loess Plateau, Ministry of Agriculture, Northwest A&F University, Yangling, Shaanxi 712100, China

ARTICLE INFO

Keywords:
Apolipoprotein D
Desiccation tolerance
Fecundity
Hydrocarbon
Acyrthosiphon pisum

ABSTRACT

Apolipoprotein D (ApoD) is a lipocalin superfamily member that plays important roles in the transport of small hydrophobic molecules, lipid metabolism, and stress resistance. Cuticular hydrocarbons are the principal components of the epicuticular lipid layer and play a critical role in water retention against environmental desiccation stress; however, the mechanism underlying the role of ApoD in insect desiccation tolerance has not yet been elucidated. Here, we report the molecular constitution, functional analysis, and phylogenetic relationship of the ApoD gene in *Acyrthosiphon pisum* (*ApApoD*). We found that *ApApoD* was transcribed throughout the life cycle of *A. pisum*, but was prominently expressed in the embryonic period and abdominal cuticle. In addition, we optimized the dose and silencing duration of RNAi, observing that RNAi against *ApApoD* significantly reduced the levels of both internal and cuticular hydrocarbons and adult fecundity. Moreover, cuticular hydrocarbon deficiency increased the sensitivity of aphids to desiccation stress and reduced their survival time, while desiccation stress significantly increased *ApApoD* expression. Together, it is confirmed that *ApApoD* participates in regulating cuticular hydrocarbon content of aphids under desiccation stress and is crucial for aphid reproduction. Therefore, the *ApApoD* gene of *A. pisum* may be a potential target for RNAi-based insect pest control due to its involvement in cuticular hydrocarbon accumulation and reproduction.

1. Introduction

The lipocalin protein superfamily consists of a large number of small extracellular proteins (Flower, 1996) with high sequence diversity that play multi-functional roles as transport proteins in retinol transport, odorant and pheromone transport, and prostaglandin biosynthesis. In addition, lipocalins can maintain homeostasis, modulate the immune response, and act as carrier proteins in the clearance of endogenous and exogenous compounds (Flower, 1996).

Apolipoprotein D (ApoD) is an extracellular glycosylated lipocalin that was first isolated from the plasma of humans (Jarrier et al., 1963) and has since been shown to be an important protein for internal circulation in insects due to its role in lipid transport (Chen et al., 2016b). As a component of high-density lipoproteins (HDLs), ApoD is mainly carried by HDLs in plasma, but can also be found in very low- and low-density lipoproteins (VLDLs and LDLs, respectively) (Goessling and Zucker, 2000) and has been implicated in the transport of cholesterol and other lipids. In some insects, HDLs accept and deliver lipids from one tissue to another as a reusable carrier, mainly transporting hydrophobic lipids, such as carotenoids, cholesterol, diacylglycerol, hydrocarbons (HCs), and phospholipids (Fan et al., 2004). In addition to binding and transporting specific hydrophobic molecules (McConathy and Alaupovic, 1973), including bilirubin, pregnenolone (Pearlman et al., 1973), progesterone, cholesterol (Peitsch and Boguski, 1990), arachidonic acid (Morais Cabral et al., 1995), E-3-methyl-2-hexenoic acid (Zeng et al., 1996), as well as retinol (Newcomer and Ong, 2000), ApoD also participates in several biological anti-stress processes by exerting anti-oxidative and anti-inflammatory functions (Bhatia et al., 2012; Tsukamoto et al., 2013; Zhou et al., 2020).

Two ApoD homologs have been shown in *Drosophila melanogaster*, namely neural lazarillo (NLaz) and glial lazarillo (GLaz) (Sánchez et al., 2000). GLaz is similar to human ApoD (40% identity) (Walker et al., 2006) and its mutagenesis decreases life span and accelerates neurodegeneration (Sanchez et al., 2006), whereas its overexpression

* Corresponding authors.
E-mail addresses: jianwen.qiao@nwafu.edu.cn (J.-W. Qiao), yfan@nwafu.edu.cn (Y.-L. Fan), wubingjin2017@nwafu.edu.cn (B.-J. Wu), wanghande@yahoo.com (D. Wang), txliu@nwafu.edu.cn (T.-X. Liu).
[1] These authors contributed equally to this work.

https://doi.org/10.1016/j.jinsphys.2020.104160
Received 21 September 2020; Received in revised form 27 October 2020; Accepted 28 October 2020
Available online 30 October 2020

increases mean life span, stress resistance against starvation, and different forms of oxidative stress (Walker et al., 2006). NLaz exerts functions that include protection against oxidative stress, longevity, and metabolic regulation (Hull-Thompson et al., 2009; Ruiz et al., 2011); however, the two homologs exhibit sex differences (Ruiz et al., 2011). In *D. melanogaster,* the functional replacement of NLaz with lazarillo (Laz), an ApoD homolog from the American grasshopper *Schistocerca americana*, has been shown to increase *Drosophila* longevity and stress resistance, including starvation-desiccation resistance (Ruiz et al., 2012). Moreover, it has been shown that ApoD1 of *Bombyx mori* (*BmApoD1*) is significantly upregulated in larvae after oxidant and starvation treatment, while the recombinant BmApoD1 protein can protect cells from H_2O_2-induced oxidative stress and reduce actinomycin D-induced apoptosis (Zhou et al., 2020, 2018). Therefore, the functions of many ApoD, NLaz, and Laz proteins have been conserved during evolution and are critical for metabolic adaptation to environmental challenges.

Cuticular hydrocarbons (CHCs) protect against environmental stress in insects (Otte et al., 2018), particularly terrestrial species. Given their large surface area-to-volume ratio, terrestrial insects face a risk of desiccation when exposed to low humidity and/or high temperatures (Chown et al., 2011); therefore, maintaining water balance is critical for their survival, and the major route via which water loss is controlled is the cuticle (Chung and Carroll, 2015). Insect CHCs are synthesized in large ectodermally-derived cells known as oenocytes (Chen et al., 2020; Diehl, 1973; Fan et al., 2003; Lawrence and Johnston, 1982; Makki et al., 2014; Schal et al., 1998; Wigglesworth, 1970) and are a complex blend of long-chain alkanes, alkenes, and methyl-branched derivatives (Arcaz et al., 2016; Blomquist, 2010; Pei et al., 2019). These CHCs act as waterproofing agents to prevent desiccation (Gibbs, 1998; Ingleby, 2015; Otte et al., 2018), play major roles in chemical communication, and serve as semiochemicals (Bontonou et al., 2013; Chung and Carroll, 2015; Ferveur, 2005; Howard and Blomquist, 2005).

Aphids (Hemiptera: Aphididae) are prevalent agricultural crop pests worldwide that reduce the economic value of crops and cause huge economic loss by exclusively ingesting the phloem sap of plants and transmitting numerous viral plant pathogens (Dedryver et al., 2010; Ng and Perry, 2004). Due to their phenotypic plasticity and super adaptability to the environment, aphids are difficult to control (Simon and Peccoud, 2018). Current aphid control strategies involve the extensive use of chemical insecticides, which lead to unacceptable environmental pollution and the emergence of insecticide-resistant aphids (Niu et al., 2019). As many pesticides can threaten human health and the environment, RNAi is emerging as an eco-friendly, efficient, and reliable method for pest control (Mamta et al., 2016). Although the genomic data of *A. pisum* has offered a foundation for studying gene function (Consortium, 2010), no studies have yet investigated *ApApoD* in *A. pisum* and its role in tolerance to desiccation stress and adult reproduction.

In the current research, we performed molecular characterization of *ApApoD* and examined its functional role with respect to aphid desiccation tolerance and fecundity. We found that *ApApoD* knockdown significantly decreased the content of internal HCs (IHCs) and CHCs, and adult fecundity. Together, the results indicate that *ApApoD* is necessary for the desiccation tolerance and fecundity of aphids and identify *ApApoD* as a potential target for aphid management.

2. Materials and methods

2.1. Pea aphids

A clonal pea aphid culture was derived from a single parthenogenetic female in Gansu Province, China and maintained on broad bean (*Vicia faba* L.) seedlings under controlled conditions of 18 °C, ~70% relative humidity (RH), and a 16L:8D light cycle in a climate chamber. To harvest developmentally synchronized aphids, newborn first-instar nymphs were collected from adult females within 12 h and placed on fresh plants. Second, third, and fourth nymphal instars and adults were respectively harvested on days 4, 6, 8, and 10 after collection. The third-instar nymphs have been chosen for RNAi experiments.

2.2. ApoD sequence analysis, structural comparison, and phylogenetic analysis

ApApoD was obtained from the protein database of *A. pisum* using the amino acid sequence of the GLaz gene (A1Z991), an ApoD homolog in *D. melanogaster*, which was obtained from UniProtKB. Bioinformatics analyses were carried out using Gene Structure Display Server (GSDS) V2.0 online (http://gsds.cbi.pku.edu.cn/) and Illustrator for Biological Sequences (IBS) V1.0.3. The functional ApoD domains from *A. pisum* and other representative insects, including *Anopheles gambiae* (*AgApoD*, Q7Q9I2), *Blattella germanica* (*BgApoD*, A0A2P8YJV8), *B. mori* (*BmApoD*, H9J5L4), *D. melanogaster* (*DmApoD*, A1Z991), *Helicoverpa armigera* (*HaApoD*, I3UIH6), and *Nilaparvata lugens* (*NlApoD*, A0A1I9WL92), were obtained from SMART website (http://smart.embl-heidelberg.de/).

To investigate the evolutionary relationship between ApoD from *A. pisum* and other insects, an evolutionary tree was reconstructed using MEGA V10.0.5 with the neighbor-joining (NJ) method (accession numbers of the protein sequences presented in Table S1). Amino acid sequence alignment was carried out by MUSCLE in MEGA with default parameters. NJ amino acid analysis was implemented in MEGA-X V10.0.5 with a Poisson model and 1000 bootstrap replicates.

2.3. Tissue dissection, RNA isolation, cDNA synthesis, and cloning

Six body parts and tissues including head, thorax, abdomen, abdominal integument, gut, and embryo (late embryonic period) were dissected from adults. All samples were collected with three biological replicates for RNA isolation. RNAiso Plus reagent (TaKaRa Bio, Kusatsu, Japan) was used to extract total RNA from each sample, and then 800 ng total RNA was reverse transcribed to cDNA using a PrimeScript™ RT Reagent Kit (TaKaRa Bio). A pair of specific primers (10 μM) was synthesized to amplify the 300-bp fragment of *ApApoD* (Table S2). Lymphotoxin A of *Mus musculus* (*Muslta*; XM_006536550.2) was used as a control gene not found in *A. pisum* (Chen et al., 2016a). A list of sequences of gene-specific primers is shown in Table S2. The reaction volume for PCR amplification was 25 μL, containing 1 μL of cDNA, 2 μL of specific primers, 0.1 μL of Ex Taq (TaKaRa Bio), 2 μL of dNTP mixture, 2.5 μL of 10 × Ex Taq Buffer, and 17.4 μL of double-distilled water. The PCR cycling conditions were as follows: initial denaturation at 94 °C for 3 min, 40 cycles of 94 °C for 30 s, 60 °C for 30 s, and 72 °C for 20 s, and a final extension at 72 °C for 5 min. PCR fragments were gel-purified using a Gel DNA Extraction Kit (TaKaRa Bio) and cloned into the pMD™19-T vector (TaKaRa Bio).

2.4. Quantitative reverse transcription PCR (RT-qPCR)

ApApoD expression levels were quantified by RT-qPCR using SYBR® Premix Ex Taq™ II (TaKaRa Bio) on an ABI 7300 Real-Time PCR System (Bio-Rad Laboratories, Hercules, CA, USA). Ribosomal protein S20 (*Rps20*; NM_001162819.2), the *A. pisum* housekeeping gene, was used as an internal control, as described by (Qiao et al., 2020). Relative target gene expression was calculated as Ct values normalized to *Rps20* using the mathematical model of Pfaffl (2001) and REST 2009 software (Qiagen, Hilden, Germany). Three biological replicates and three technical replicates were used for each treatment.

2.5. dsRNA synthesis and delivery

dsRNA was synthesized using a 300-bp coding fragment of *ApApoD* designed as an RNAi target region. Only one RNAi target was designed because the *ApApoD* coding sequence (CDS) is small (just 585 bp) and ds*Muslta* (193 bp) was used as a negative control. The target fragment was amplified using a resultant plasmid, with targets gene sequence-

specific primers containing T7 promoters as templates for dsRNA synthesis (Table S2). dsRNA was transcriptionally synthesized and purified using a T7 RiboMAX™ Express RNAi System (Promega, Madison, WI, USA) according to the manufacturer's instructions. The integrity of dsRNA was detected on agarose gel, and then dsRNA was quantified and adjusted to a working concentration (6 μg/μL). All dsRNAs were stored at − 80 °C for further use. dsRNA was delivered via body microinjection as described previously (Qiao et al., 2020). Briefly, third-instar nymphs were fixed to the sticky end of a Post-it Note and purified dsRNAs were injected into the suture between the ventral mesothorax and metathorax using the Nanoject II micro-injector apparatus (Drummond Scientific, Broomall, PA).

2.6. Rnai efficiency determination

To optimize the *ApApoD* dose for RNAi, 50.6, 101.2, 151.8, 202.4, 253, and 303.6 nL of the dsRNAs (6 μg/μL) were injected into third-instar nymphs, and suppression efficiency was checked on the second day after injection. To confirm the duration of effective RNAi for the optimal dose selected, aphids were collected at each time point from 1 to 6 days after injection for RNAi efficiency determination. Each sample containing five aphids was evaluated for RNAi efficiency by RT-qPCR.

2.7. HC extraction and quantification

Third-instar nymphs injected with ds*ApApoD* or ds*Muslta* were transferred to new plants for 3 days and their HC levels were quantified. To extract CHCs, 200 ng of *n*-tetracosane (only once) was added to each sample containing four nymphs (about 10 mg fresh weight) as an internal standard, and then the samples were immersed in 200 μL of *n*-hexane and agitated gently for 2 min. This extraction step was repeated twice. The hexane extracts were collected in a new vial and reduced to ~ 300 μL using a gentle stream of high-purity N_2. Then, the concentrated hexane extracts were purified using a ~ 300 mg silica gel mini column in a glass wool-stoppered Pasteur pipette and 2 mL of hexane was added to elute the HC fraction. Finally, the eluent was dried under N_2 and resuspended in 50 μL of hexane for measurement.

IHCs and CHCs were collected from the same aphids. First, 200 ng of *n*-tetracosane was added as an internal standard and the aphids were homogenized in 300 μL of double-distilled water, and then mixed with 2 mL of hexane:methanol:water (2:1:1). After vigorous vortexing for 1 min, the mixture was incubated undisturbed overnight at 25 ± 1 °C. Next, centrifugation was performed at 2000*g* for 10 min, and ~ 500 μL of the hexane phase (top layer) was moved to a vial, purified, and prepared for gas chromatography analysis.

The quantification of hydrocarbon was performed using a TRACE 1310 (Thermo Fisher Scientific) gas chromatograph (GC) connected with a mass spectrometer (MS). Helium as the carrier gas maintained at a constant flow rate of 1 mL/min with 1 μL splitless injection into a 30 m × 0.32 mm × 0.25 μm HP-5MS UI capillary column (Agilent Technologies, Santa Clara, CA, USA). The running program was operated at 60 °C for 2 min followed by 5 °C/min to 320 °C and holding for 10 min. The temperatures of injector and detector are 300 °C and 280 °C, respectively.

2.8. Desiccation tolerance bioassay

To analyze *ApApoD* expression, third-instar nymphs were transferred to desiccation environment. Fifty aphids and 10 g of fresh allochroic silica gel were put into a 50-mL tube separated by an absorbent cotton stopper and the tube was sealed with Parafilm. The RH above the tube dropped to 5% within 60 min as monitored by a HOBO Pro v2 Data Logger (Onset Computer Corporation, Bourne, MA, USA). In the control group, fifty aphids were transferred to a tube but without the desiccant. The two tubes were then put in a climate chamber at 18 °C, ~70% RH, and a 16:8h (light:dark) photoperiod. *ApApoD* expression levels were detected by RT-qPCR after 24 and 48 h.

To observe dehydration tolerance, at least thirty ds*ApApoD*-injected aphids were exposed to desiccation (<5% RH) at 18 °C on the second day after dsRNA injection, with the same number of ds*Muslta*-injected aphids as the control group. Every 6 h, the number of surviving aphids was counted.

2.9. Fecundity evaluation

At least thirty third-instar nymphs of each group injected with ds*ApApoD* or ds*Muslta* were placed on plants in a chamber (18 °C, ~70% RH, and light–dark 16:8). After the emergence of newborn nymphs, cumulative average reproduction was noted every 12 h until accumulated 120 h. Embryos were counted and photographed from at least 15 aphids per group using a microscope 72 h after dsRNA injection.

2.10. Statistical analysis

Statistical analyses were performed using the SPSS V22.0 software (IBM, Armonk, NY, USA). Significance testing of two and multiple samples were implemented using Student's *t*-tests and one-way analysis of variance (ANOVA), respectively.

3. Results

3.1. ApApoD molecular characterization, RNAi, and phylogenetic analysis

ApApoD (J9KFX7) was found to exhibit 40.6% identity with the *D. melanogaster* GLaz gene (A1Z991) at the amino acid level (Fig. 2A). The full length *ApApoD* mRNA spliced from four exons was 1607 bp (Fig. 1A), including a 526 bp 5′-untranslated region (UTR) and 660 bp 3′-UTR (Fig. 1B). *ApApoD* encodes a protein of 194 amino acids containing a 21 amino acid signal peptide and a 148 amino acid lipocalin domain (Fig. 1C). The RNAi target region (300 bp) and qPCR detection region (83 bp) were designed from the *ApApoD* CDS region in a mutually independent manner (Fig. 1B).

Functional domain analysis confirmed that *ApApoD* encoded ApoD as it shared the characteristic domain of insect ApoD, which contains a signal peptide and lipocalin domain (Fig. 2A). Phylogenetic analysis revealed the evolutionary relationship between *ApApoD* and other insect ApoDs (Fig. 2B). *ApApoD* grouped together with ApoDs from *Schizaphis graminum*, *Cinara cedri*, and *Sipha flava*, indicating a close ancestry compared to other insect ApoDs; however, the ApoD genes were not significantly conserved in insects (Fig. 2A and B).

3.2. ApApoD expression profile

The expression profile of *ApApoD* in different developmental stages, body segments, and tissues of aphids was analyzed by RT-qPCR. *ApApoD* was expressed in all developmental stages ($F_{5,\ 12} = 48.460$, $P < 0.0001$; Fig. 3A); however, *ApApoD* was expressed at significantly higher levels during the embryonic stage than at other nymph and adult stages. *ApApoD* expression was maintained at a similar level from first-instar nymphs through to the adult stage, with the exception of significantly up-regulated expression at the first- and third-instar periods. We also analyzed mRNA expression level of *ApApoD* in different tissues and body segments ($F_{4,\ 10} = 115.597$, $P < 0.0001$; Fig. 3B), finding that *ApApoD* expression was the highest in the abdominal integument and was higher in the head and abdomen than in the thorax and gut, which had the lowest *ApApoD* expression.

3.3. Effect of desiccation on ApApoD expression

In third-instar nymphs, mRNA abundance of *ApApoD* under desiccation stress were analyzed by qRT-PCR after 24 and 48 h (Fig. 4).

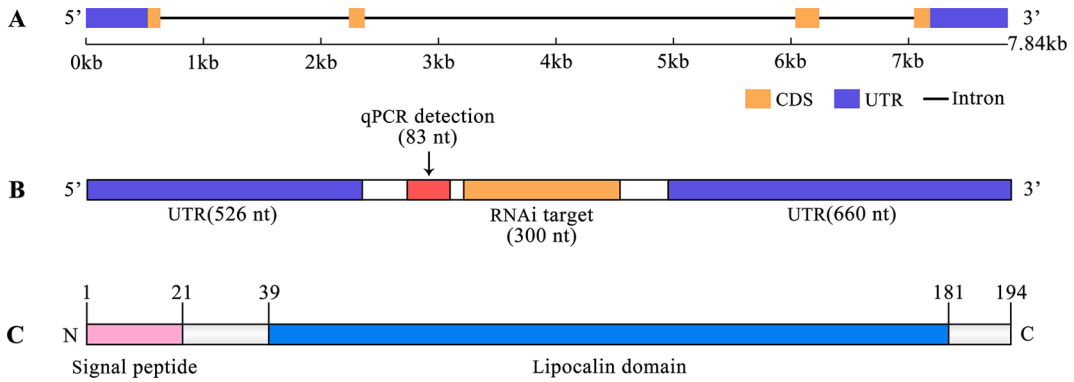

Fig. 1. Sequence analysis of *A. pisum* apolipoprotein D (*ApApoD*). (A) *ApApoD* 5′-untranslated region (UTR), coding sequence (CDS), intron, and 3′-UTR organization were analyzed via a comparison in transcripts and genomic data. (B) Schematic diagram of RNAi against *ApApoD* mRNA. Different colors indicate the RNAi target area and a non-overlapping qPCR detection region from the CDS. (C) Putative amino acid sequence including the characteristic signal peptide and lipocalin domain are highlighted with different colored boxes.

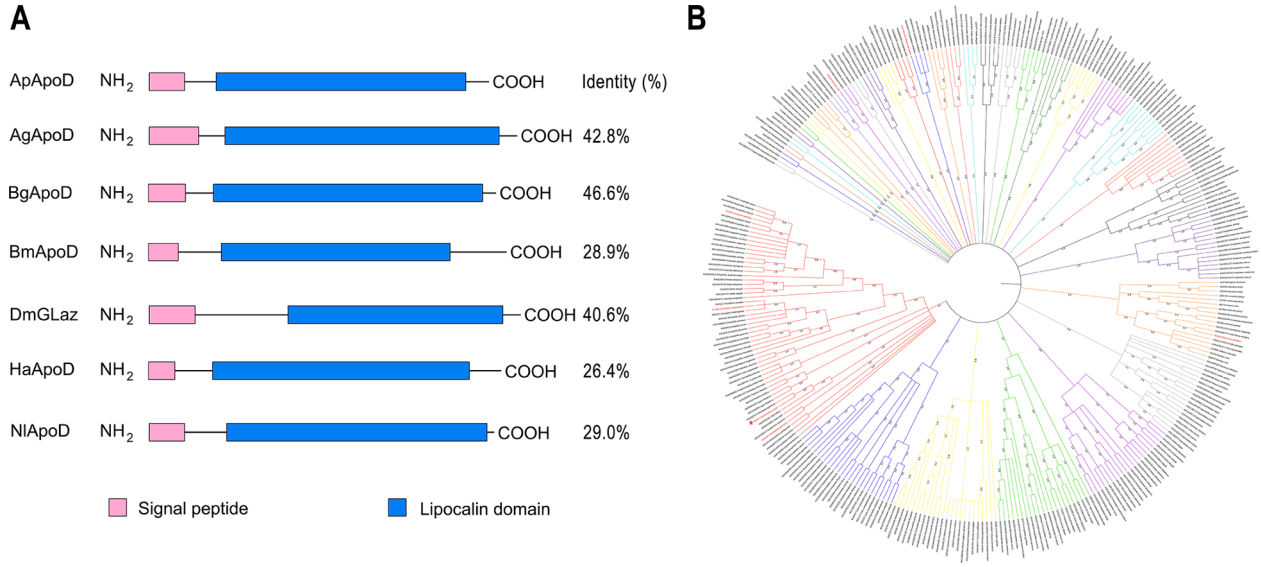

Fig. 2. Sequence analysis of apolipoprotein D (ApoD) and its homologs. (A) Schematic diagram of the modular domains of *A. pisum* ApoD (*ApApoD*) and its homologs from representative insects: *Acyrthosiphon pisum* (*ApApoD*, J9KFX7), *Anopheles gambiae* (*AgApoD*, Q7Q9I2), *Blattella germanica* (*BgApoD*, A0A2P8YJV8), *Bombyx mori* (*BmApoD*, H9J5L4), *Drosophila melanogaster* (*DmGLaz*, A1Z991), *Helicoverpa armigera* (*HaApoD*, I3UIH6), and *Nilaparvata lugens* (*NlApoD*, A0A1I9WL92). Identity values (%) mean that similarity of ApoD protein sequence between *A. pisum* and other insects. (B) Phylogenetic analysis between ApoD and its homologs from insects. *ApApoD* and six other representative insect ApoDs or homologs from Fig. 2A are indicated in red. The *ApApoD* sequence from this study is marked with a red asterisk. (For interpretation of the references to colour in this figure legend, the reader is referred to the web version of this article.)

ApApoD expression was significantly up-regulated by 1.21-fold ($P < 0.003$) compared with the control group (70% RH) after 24 h of desiccation (<5% RH) and was up-regulated by 1.48-fold as the duration of desiccation increased to 48 h ($P < 0.0001$).

3.4. ApApoD knockdown by dsRNA injection

The optimal suppression dosage of *ApApoD* was confirmed by adjusting the injection volume of dsRNA (6 μg/μL) (Fig. 5A). Increasing the injection dose gradually increased the *ApApoD* RNAi efficiency to a maximum of 88.5% ($P < 0.0001$) at 1.21 μg, with the efficiency decreasing when the dose was increased to 1.52 and 1.82 μg. At these doses, mRNA inhibition was maintained at approximately 60%, with no significant difference being observed in RNAi efficiency. Therefore, the optimal ds*ApApoD* dose for RNAi was determined to be about 1.21 μg per aphid.

During the 6 days following dsRNA injection into the aphids, *ApApoD* transcript levels first decreased and then increased (Fig. 5B). RNAi efficiency against *ApApoD* increased from 50.8% ($P < 0.006$, day 1) to a maximum of 70.1% ($P < 0.0001$, day 2), then gradually decreasing to 16.6% ($P < 0.04$, day 5). On the sixth day, there was no significant difference in *ApApoD* levels.

3.5. Effect of ApApoD knockdown on HC levels

Next, HC content in aphids injected with ds*ApApoD* was quantified by GC–MS. Suppressing *ApApoD* expression reduced external and internal HC levels by 22.4% ($P < 0.0001$) and 28.1% ($P < 0.001$), respectively (Figs. 6A and 7A). Additionally, GC–MS analysis revealed that aphid CHCs were composed of nine C_{25}–C_{33} *n*-alkanes (Table S3), nevertheless their IHCs consisted of 24*n*-alkanes and their methyl-branched alkanes (Table S4). To confirm the effect of *ApApoD* suppression on the content of these nine CHC *n*-alkanes, the mean values of each *n*-alkane per aphid were compared with the controls (Fig. 6B). In the ds*ApApoD*-injected group, C_{25}, C_{28}, C_{29}, C_{30}, C_{31}, C_{32}, and C_{33} levels decreased significantly by 21.2, 10.7, 18.5, 42.7, 37.4, 63.3, and 49.8%,

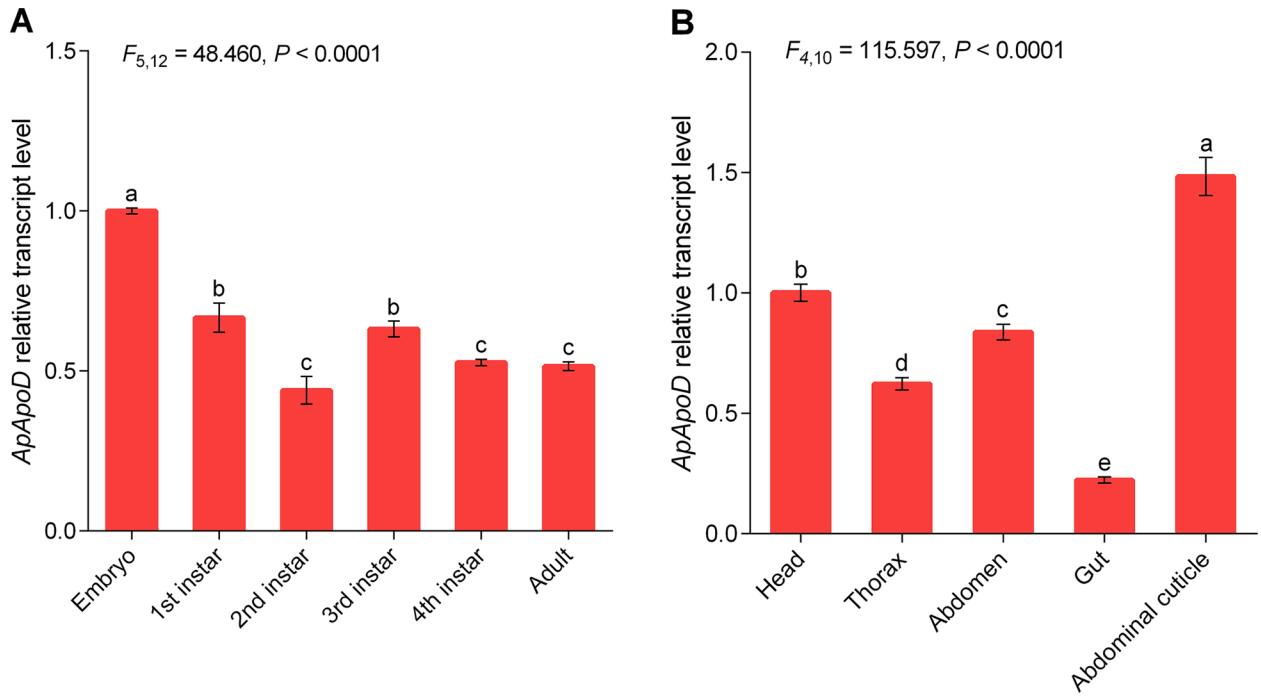

Fig. 3. Spatiotemporal expression analysis of *A. pisum* apolipoprotein D (*ApApoD*). (A) Relative *ApApoD* expression at various stages of development. The embryos (n = 50), adults (n = 5), 1st- (n = 40), 2nd- (n = 20), 3rd- (n = 10), and 4th-instar aphids (n = 8) were collected for detection. (B) *ApApoD* abundance in various tissues. RNA was extracted from gut (n = 50), head (n = 40), abdominal cuticle (n = 20), thorax (n = 10), and abdomen (n = 10). Data represent the mean ± standard error in triplicate. The different lower-case letters above bars show significant differences (One-way ANOVA, P < 0.05).

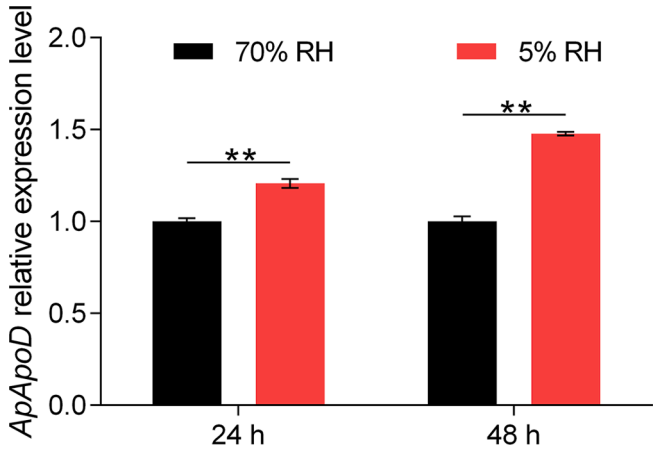

Fig. 4. The influence of desiccation on *A. pisum* apolipoprotein D (*ApApoD*) expression. The third-instar aphids were exposed to desiccation environment for 24 and 48 h; 70% RH was chosen as control. RH denotes relative humidity. Data show the mean ± standard error in triplicate. **P < 0.01 (Student's t-test).

respectively; however, C_{26} and C_{27} levels did not significantly differ between the ds*ApApoD*-injected groups and the control.

The mean values of every IHC compound per aphid were also compared to those in the control aphids (Fig. 7B), revealing that levels of all 15 methyl-branched alkanes in the ds*ApApoD*-injected group were significantly lower than those in control, with the largest reduction for x, x-diMeC_{32} (67.6%). Among the nine internal n-alkanes, n-C_{25}, n-C_{27}, and n-C_{30} levels decreased significantly by 22.2, 35.4, and 31.3%, respectively. No significant differences were observed in the n-C_{26}, n-C_{28}, n-C_{32}, and n-C_{33} contents between the ds*ApApoD*-injected group and the control group; however, n-C_{29} and n-C_{31} levels increased significantly by 31.1 and 51.3%, respectively. Figs. S1 and S2 respectively display the CHC and IHC chromatograms of aphids injected with ds*ApApoD* and ds*Muslta*.

3.6. Effect of desiccation on the survival rate of dsApApoD-injected aphids

Next, the survival of aphids was investigated after *ApApoD* mRNA was suppressed under desiccation stress (Fig. 8A). The *ApApoD* suppression increased aphid sensibility to dehydration environment and significantly decreased their survival rate after 6 h compared to the control group (P < 0.0001). Moreover, ds*ApApoD* injection significantly decreased the survival rate by 95.5% after 24 h, with all ds*ApApoD*-injected aphids dying within 30 h but all ds*Muslta*-injected aphids dying within 48 h.

3.7. Effect of ApApoD suppression on fecundity

Finally, the cumulative average reproduction of *ApApoD*-inhibited aphids was analyzed (Fig. 8B), showing that new nymphs of aphids injected with ds*ApApoD* were produced 24 h later compared with the control aphids. Indeed, the cumulative average reproduction of *ApApoD*-inhibited aphids was significantly less than control from 24 to 120 h, with the control ds*Muslta*-injected aphids exhibiting strong fecundity and the ds*ApApoD*-injected aphids exhibiting weak fecundity.

Embryos of *ApApoD*-suppressed aphids were observed to confirm the effect of *ApApoD* knockdown on fecundity (Fig. 8C and D). *ApApoD*-suppressed aphids produced approximately 9 embryos, compared to the 16 produced per control aphid on average (i.e., 40.14% decrease). In addition, embryonic development of aphids injected with ds*ApApoD* was retarded, whereas embryos of control aphids injected with ds*Muslta* exhibited full development and maturity.

4. Discussion

In the present study, we identified and characterized an *ApApoD* gene from *A. pisum*, and explored its function using RNAi. Results showed that

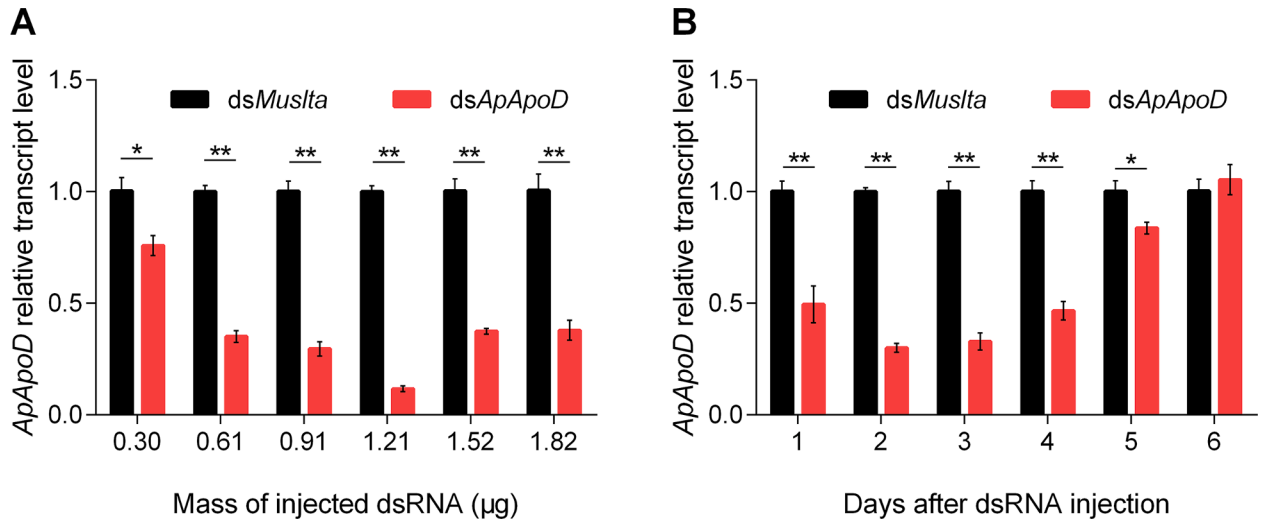

Fig. 5. The influence of RNAi suppression on *A. pisum* apolipoprotein D (*ApApoD*) expression. (A) *ApApoD* transcript dose–response in third-instar nymphs to microinjection with a series of dsRNA doses (0.30–1.82 μg). RNAi efficiency was detected 48 h after injection. (B) At the optimal dosage (1.21 μg), the effect of RNAi varied with duration. Third-instar nymphs after injection were detected for six days. Data represent the mean ± standard error in triplicate. $^{*}P < 0.05$; $^{**}P < 0.01$ (Student's *t*-test).

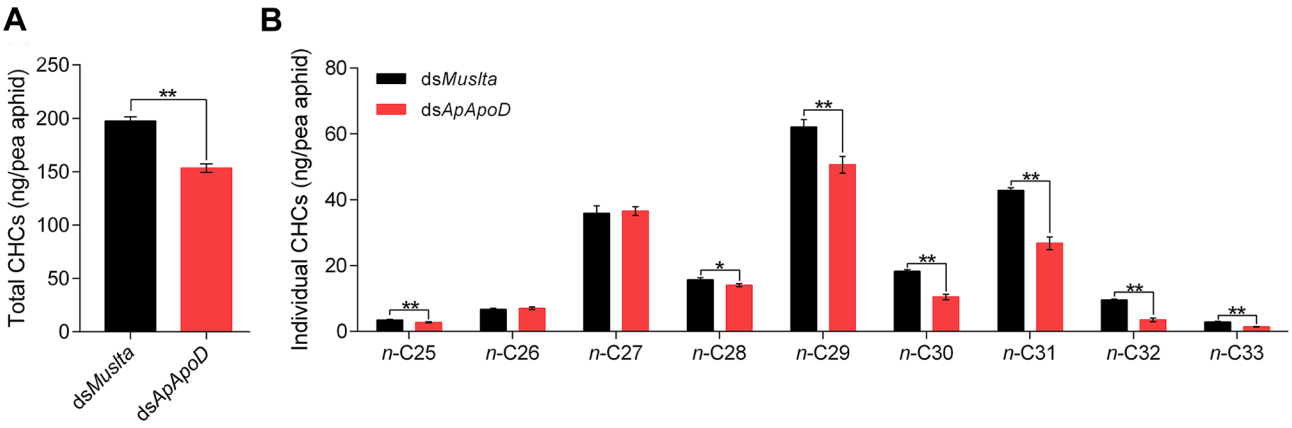

Fig. 6. Effect of *A. pisum* apolipoprotein D (*ApApoD*) RNAi on CHCs in *A. pisum*. Third-instar aphids after dsRNA injection were transferred to new seedlings for three days, and CHC levels were quantified. (A) The contents of total CHC of aphids injected with dsRNA. (B) Quantification of nine CHCs of aphids injected with dsRNA. The calculated values are listed in Table S3. See Fig. S1 for the CHC gas chromatograms. Data represent the mean ± standard error of five biological replicates. $^{*}P < 0.05$; $^{**}P < 0.01$ (Student's *t*-test).

HC content correlated positively with *ApApoD* abundance, while *ApApoD* knockdown by RNAi decreased HC content and increased aphid sensitivity to desiccation. As far as we know, this is the first functional study of ApoD in a hemipteran insect species.

ApoD has been shown to have many important functions in key processes, such as stress responses, longevity regulation, and lipid metabolism (Muffat et al., 2008; Rassart et al., 2020; Ruiz et al., 2012; Sanchez et al., 2006; Walker et al., 2006; Zhou et al., 2020, 2018). The results of this study are consistent with the conservative regulation and function of ApoD and its homologs under stress conditions, with desiccation stress significantly increasing *ApApoD* expression over time. In addition, *ApApoD* silencing significantly reduced the survival time of aphids under desiccation stress, indicating a positive relationship between *ApApoD* expression and desiccation tolerance. This conclusion is consistent with a previous study, which showed that *Drosophila* overexpressing the ApoD homolog *GLaz* lived 30% longer than control flies under desiccation (Walker et al., 2006). Similarly, when the ApoD homolog *NLaz* secreted by *Drosophila* was functionally replaced with *Grasshopper Laz*, *Laz* overexpression increased survival rate (23.1.30% median increase) upon desiccation stress (Ruiz et al., 2012). Together with our findings, these studies indicate that insect ApoD and its homologs are involved in desiccation tolerance.

Insect desiccation tolerance is primarily regulated by long-chain HCs, which are essential waterproofing components present on the epicuticle of insects (Qiu et al., 2012). Due to the positive relationship between *ApApoD* and desiccation tolerance, we quantified CHC content and found that *ApApoD* silencing significantly reduced the CHC content of aphids, suggesting that *ApApoD* may regulate desiccation tolerance in *A. pisum* by modulating CHC production. The ApoD protein plays a key role in the internal circulation of insects via lipid transport (Chen et al., 2016b) as it can bind and transport specific hydrophobic molecules (McConathy and Alaupovic, 1973) using an eight-stranded antiparallel β-barrel with a ligand-binding pocket (Flower et al., 2000). Therefore, we speculate that *ApApoD* may also be involved in the transport of HC precursors or HCs associated with HDL. Previously, Schal et al. (1998) reported that HC levels are usually constant in *B. germanica* and are supplemented by IHCs if necessary; therefore, blocking HC transport and deposition in RNAi-suppressed aphids may only change IHC levels at first, with CHC levels decreasing after a substantial reduction in IHC levels. This hypothesis is consistent with our results; despite a significant

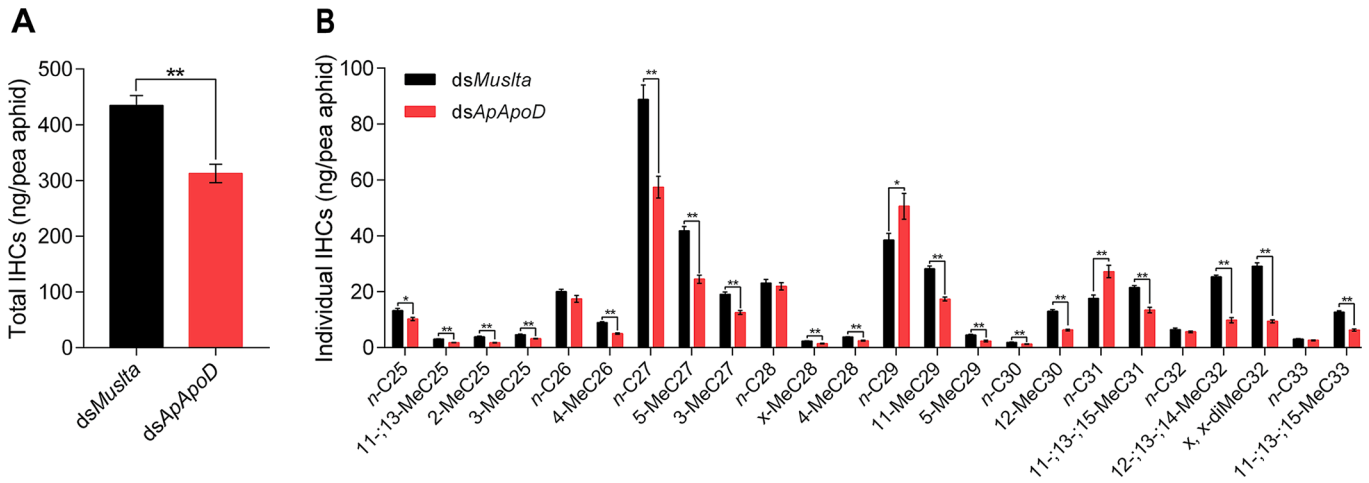

Fig. 7. The influence of the internal hydrocarbons (IHCs) contents of *A. pisum* following dsRNA injection. Third-instar aphids after dsRNA injection were transferred to new seedlings for three days, and IHC levels were quantified. (A) The contents of total IHC of aphids injected with dsRNA. (B) Quantification of 24 IHCs of aphids injected with dsRNA. The calculated values are shown in Table S4. See Fig. S2 for the IHC gas chromatograms. Data represent the mean ± standard error of five biological replicates. $^{*}P < 0.05$; $^{**}P < 0.01$ (Student's *t*-test).

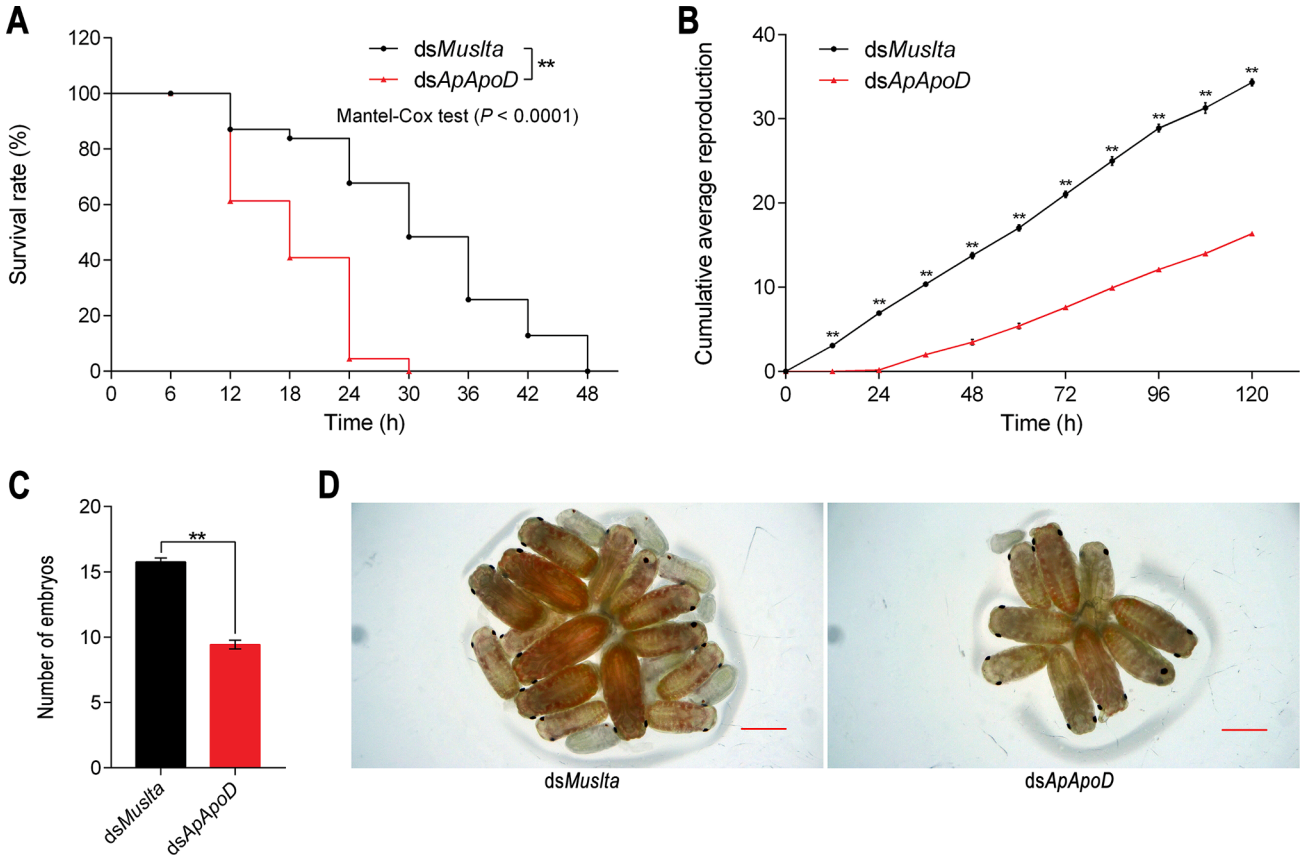

Fig. 8. The influence of *A. pisum* apolipoprotein D (*ApApoD*) suppression on desiccation tolerance and adult fecundity in *A. pisum*. Third-instar nymphs after dsRNA injection were transferred to new seedlings to biologically evaluate desiccation tolerance and fecundity. (A) Effect of desiccation on the survival rate of aphids two days post injection of ds*ApApoD* or ds*Muslta*; $n = 30$ aphids (at least). *P* value was derived by the Mantel-Cox test. (B) Record of cumulative average reproduction; $n = 30$ aphids (at least). The values were calculated from three biological replicates (means ± standard error). $^{**}P < 0.01$ (Student's *t*-test). Number (C) and photos (D) of embryos dissected from aphids 72 h after ds*ApApoD* or ds*Muslta* injection. $n = 15$ aphids (at least). Data represent the mean ± standard error in triplicate. $^{**}P < 0.01$ (Student's *t*-test). Red scale bars in illustration D = 0.5 mm. (For interpretation of the references to colour in this figure legend, the reader is referred to the web version of this article.)

reduction in both CHC and IHC levels due to *ApApoD* silencing, IHC levels displayed a higher reduction than did CHCs. In insects, HCs are transported mainly by the HDL lipophorin (Fan et al., 2004); however, it is not yet known how *ApApoD* interacts with lipophorin and this relationship requires further investigation. Our finding that *ApApoD* was highly expressed in the abdominal cuticle suggests that *ApApoD* is

related to the accumulation of tissue-specific CHC. Therefore, we concluded that *ApApoD* is involved in HC transport, but the underlying mechanisms warrant further investigation.

Our study also found that *ApApoD* was highly expressed in embryos, indicating that *ApApoD* may be associated with aphid reproduction. Compared to the ds*Muslta*-injected control aphids, the *ApApoD*-silenced aphids exhibited retarded embryo development, fewer embryos, delayed nymph production, and lower cumulative average reproduction. Consistently, the absence of the two ApoD homologs, *GLaz* and *NLaz*, in *Drosophila* has been shown to reduce fecundity (Ruiz et al., 2011). Furthermore, the interaction between ApoD and retinoic acid (RA) is required for neuronal differentiation in culture, and *Drosophila NLaz* was found to successfully transport RA to immature neurons, thereby promoting neurite outgrowth (Ruiz et al., 2013). Given that *GLaz* mRNA is detected very early in embryogenesis (0–2 h embryos), the failure of *GLaz* mutant *Drosophila* eggs to reach adulthood might be due to developmental problems (Ruiz et al., 2011; Sánchez et al., 2000). Therefore, the reduced fecundity of adult aphids and delayed embryo development caused by *ApApoD* silencing may be due to developmental problems regulated by *ApApoD*; however, the specific metabolic pathways via which *ApApoD* regulates fecundity in adult aphids require further investigation.

The GC–MS data collected in this study confirmed that pea aphid CHCs consisted of nine saturated alkanes (C_{25}–C_{33}) with no methyl-branched HCs, consistent with our previous study which suggested that a series of C_{25}–C_{33} *n*-alkanes constitute the CHCs in *A. pisum* (Chen et al., 2016a; Qiao et al., 2020). However, IHCs contain a large number of methyl-branched HCs, which are significantly different from CHCs. This may be the result of organs selectively accepting different HCs, but the specific mechanism is still unclear. Such as in Holomelina aurantiaca, pheromone gland and epidermal cells respectively have stringent selectivity for pheromone and long-chain HCs (Schal et al., 1998). Similarly, deposition of various lipids bound to lipophorin exhibits tissue specificity: HCs are mainly deposited in the cuticle and ovaries whereas diacylglycerols are deposited in muscles for use (Chino, 1985). In addition, we found that *ApApoD* silencing had different effects on the levels of different HC components, suggesting that *ApApoD* may be involved in the tissue-specific deposition of different HCs, just like in moths, the deposition of HC pheromone precursors are very specific in that only the pheromone is unloaded at the pheromone gland, whereas most HCs are transported to cuticular surface and they are not unloaded into the pheromone gland (Jurenka et al., 2003; Schal et al., 1998). However, further studies are required to elucidate the mechanism underlying the effect of *ApApoD* on HC deposition.

RNAi efficiency and the duration of knockdown effects are two particularly important factors for gene function studies. Previous successful RNAi experiments on pea aphids have shown that the optimal dsRNA injection dose depends on the specific target gene (Ye et al., 2019; Yu et al., 2016); therefore, we explored the optimal dsRNA injection dose for *ApApoD* and found that the most effective dose was 1.21 μg, with the RNAi efficiency not increasing above this dose. This result is similar to that of our previous study in which we identified the optimal dsRNA dose for *ApLpR*, wherein a dose exceeding the optimal dose did not increase RNAi efficiency, but exerted the opposite effect (Qiao et al., 2020). This may be due to excessive dsRNA doses inducing and increasing ribonuclease activity, thereby promoting rapid and severe dsRNA degradation and thus reduced RNAi efficiency. In terms of the duration of RNAi knockdown, our findings indicated that the effects of RNAi became apparent on the second day after dsRNA injection and that *ApApoD* could be suppressed for five days. Similarly, *cathepsin-l* gene silencing by dsRNA injection in third-instar pea aphid nymphs was found to last for 120 h (Sapountzis et al., 2014); however, *CYP4G51* and *ApLpR* silencing under the same conditions was only found to last for 72 and 96 h, respectively (Chen et al., 2016a; Qiao et al., 2020). Consequently, the duration of gene knockdown effects in pea aphids appears to differ depending on the gene. It is also difficult to achieve long-term RNAi effects in pea aphids since dsRNA can only remain intact in the hemocoel for a short period of time; therefore, it is particularly important to investigate the temporal development of silencing in aphids to provide insights for future gene function studies.

In conclusion, our findings demonstrate for the first time that *ApApoD* plays a vital role in desiccation tolerance via regulating HC content in pea aphids. Based on the shorter survival time of *ApApoD*-inhibited aphids after exposure to desiccation stress, we reveal that reduced CHC levels enhance the permeability of the cuticle and lead to accelerated water loss. Simultaneously, *ApApoD* silencing significantly reduced fecundity, revealing that *ApApoD* is important for *A. pisum* reproduction. Together, these findings may promote further biochemical research on the molecular mechanisms underlying *ApApoD* regulation during pea aphid reproduction and survival. Moreover, our study highlights that *ApApoD* may become a potential RNAi target for pest control.

Declaration of Competing Interest

The authors declare that they have no known competing financial interests or personal relationships that could have appeared to influence the work reported in this paper.

Acknowledgments

This work was done with the support of the National Natural Science Foundation of China (Grant No. 31772533) and National Key Research and Development Project (Grant No. 2018YFD0600202-03). We are grateful to Zhan-Feng Zhang (Northwest A&F University) for technical assistance on GC-MS.

Author contributions

J.Q., Y.F., T.L., and D.W. designed research; J.Q. performed research and analyzed data; B.W. provided assistance in making the figures; J.Q., Y.F., and T.L. wrote the paper.

Appendix A. Supplementary data

Supplementary data to this article can be found online at https://doi.org/10.1016/j.jinsphys.2020.104160.

References

Arcaz, A.C., Huestis, D.L., Dao, A., Yaro, A.S., Diallo, M., Andersen, J., Blomquist, G.J., Lehmann, T., 2016. Desiccation tolerance in Anopheles coluzzii: the effects of spiracle size and cuticular hydrocarbons. J. Exp. Biol. 219, 1675–1688.

Bhatia, S., Knoch, B., Wong, J., Kim, W.S., Else, P.L., Oakley, A.J., Garner, B., 2012. Selective reduction of hydroperoxyeicosatetraenoic acids to their hydroxy derivatives by apolipoprotein D: Implications for lipid antioxidant activity and Alzheimer's disease. Biochem. J. 442, 713–721.

Blomquist, G.J., 2010. Structure and analysis of insect hydrocarbons. Insect Hydrocarb. Biol. Biochem. Chem. Ecol. 19–34.

Bontonou, G., Denis, B., Wicker-Thomas, C., 2013. Interaction between temperature and male pheromone in sexual isolation in Drosophila melanogaster. J. Evol. Biol. 26, 2008–2020.

Chen, N., Fan, Y.-L., Bai, Y., Li, X.-D., Zhang, Z.-F., Liu, T.-X., 2016a. Cytochrome P450 gene, CYP4G51, modulates hydrocarbon production in the pea aphid. Acyrthosiphon pisum. Insect Biochem. Mol. Biol. 76, 84–94.

Chen, N., Pei, X.-J., Li, S., Fan, Y.-L., Liu, T.-X., 2020. Involvement of integument-rich CYP4G19 in hydrocarbon biosynthesis and cuticular penetration resistance in Blattella germanica (L.). Pest Manag. Sci. 76, 215–226.

Chen, S., Liu, M., Li, Y., Zhou, X., Hou, Y., Gong, J., 2016b. Molecular Identification and Expression Patterns of Apolipoprotein D From Bombyx mori (Lepidoptera: Bombycidae) in Response to Oxidative Stress and Bacterial Challenge. Ann. Entomol. Soc. Am. 109, 759–767.

Chino, H., 1985. Lipid transport: biochemistry of hemolymph lipophorin. Comprehensive Insect Physiology, Biochemistry and Pharmacology (eds. G.A. Kerkut & L.I. Gilbert), pp. 115–135.

Chown, S.L., Sørensen, J.G., Terblanche, J.S., 2011. Water loss in insects: An environmental change perspective. J. Insect Physiol. 57, 1070–1084.

Chung, H., Carroll, S.B., 2015. Wax, sex and the origin of species: Dual roles of insect cuticular hydrocarbons in adaptation and mating. Bioessays 37, 822–830.

Dedryver, C.-A., Le Ralec, A., Fabre, F., 2010. The conflicting relationships between aphids and men: a review of aphid damage and control strategies. C. R. Biol. 333, 539–553.
Diehl, P.A., 1973. Paraffin synthesis in the oenocytes of the desert locust. Nature 243, 468–470.
Fan, Y., Schal, C., Vargo, E.L., Bagnères, A.-G., 2004. Characterization of termite lipophorin and its involvement in hydrocarbon transport. J. Insect Physiol. 50, 609–620.
Fan, Y., Zurek, L., Dykstra, M.J., Schal, C., 2003. Hydrocarbon synthesis by enzymatically dissociated oenocytes of the abdominal integument of the German Cockroach, Blattella germanica. Naturwissenschaften 90, 121–126.
Ferveur, J.-F., 2005. Cuticular hydrocarbons: Their evolution and roles in Drosophila pheromonal communication. Behav. Genet. 35, 279–295.
Flower, D.R., 1996. The lipocalin protein family: Structure and function. Biochem. J. 318 (Pt 1, 1–14.
Flower, D.R., North, A.C., Sansom, C.E., 2000. The lipocalin protein family: Structural and sequence overview. Biochim. Biophys. Acta 1482, 9–24.
Gibbs, A., 1998. Water-Proofing Properties of Cuticular Lipids. Amer, Zool, p. 38.
Goessling, W., Zucker, S.D., 2000. Role of apolipoprotein D in the transport of bilirubin in plasma. Am. J. Physiol. Gastrointest. Liver Physiol. 279, G356–65.
Howard, R.W., Blomquist, G.J., 2005. Ecological, behavioral, and biochemical aspects of insect hydrocarbons. Annu. Rev. Entomol. 50, 371–393.
Hull-Thompson, J., Muffat, J., Sanchez, D., Walker, D.W., Benzer, S., Ganfornina, M.D., Jasper, H., 2009. Control of metabolic homeostasis by stress signaling is mediated by the lipocalin NLaz. PLoS Genet. 5, e1000460.
Ingleby, F.C., 2015. Insect cuticular hydrocarbons as dynamic traits in sexual communication. Insects. 6, 732–742.
Jarrier, M.A., Levy, G., Polonovski, J., 1963. Study of humanserum alpha-lipoproteins by immunoelectrophoresis. Bull. Soc. Chim. Biol. (Paris) 45, 703–713.
Jurenka, R.A., Subchev, M., Abad, J.L., Choi, M.Y., Fabrias, G., 2003. Sex pheromone biosynthetic pathway for disparlure in the gypsy moth, *Lymantria dispar*. Proc. Natl. Acad. Sci. USA 100, 809–814.
Lawrence, P.A., Johnston, P., 1982. Cell lineage of the Drosophila abdomen: The epidermis, oenocytes and ventral muscles. J. Embryol. Exp. Morphol. 72, 197–208.
Makki, R., Cinnamon, E., Gould, A.P., 2014. The development and functions of oenocytes. Annu. Rev. Entomol. 59, 405–425.
Mamta Reddy, K.R.K., Rajam, M.V., 2016. Targeting chitinase gene of Helicoverpa armigera by host-induced RNA interference confers insect resistance in tobacco and tomato. Plant Mol. Biol. 90, 281–292.
McConathy, W.J., Alaupovic, P., 1973. Isolation and partial characterization of apolipoprotein D: A new protein moiety of the human plasma lipoprotein system. FEBS Lett. 37, 178–182.
Morais Cabral, J.H., Atkins, G.L., Sánchez, L.M., López-Boado, Y.S., López-Otin, C., Sawyer, L., 1995. Arachidonic acid binds to apolipoprotein D: Implications for the protein's function. FEBS Lett. 366, 53–56.
Muffat, J., Walker, D.W., Benzer, S., 2008. Human ApoD, an apolipoprotein up-regulated in neurodegenerative diseases, extends lifespan and increases stress resistance in Drosophila. Proc. Natl. Acad. Sci. U. S. A. 105, 7088–7093.
Newcomer, M.E., Ong, D.E., 2000. Plasma retinol binding protein: Structure and function of the prototypic lipocalin. Biochim. Biophys. Acta 1482, 57–64.
Ng, J.C.K., Perry, K.L., 2004. Transmission of plant viruses by aphid vectors. Mol. Plant Pathol. 5, 505–511.
Niu, J., Yang, W.-J., Tian, Y., Fan, J.-Y., Ye, C., Shang, F., Ding, B.-Y., Zhang, J., An, X., Yang, L., Chang, T.-Y., Christiaens, O., Smagghe, G., Wang, J.-J., 2019. Topical dsRNA delivery induces gene silencing and mortality in the pea aphid. Pest Manag. Sci. 75, 2873–2881.
Otte, T., Hilker, M., Geiselhardt, S., 2018. Phenotypic plasticity of cuticular hydrocarbon profiles in insects. J. Chem. Ecol. 44, 235–247.
Pearlman, W.H., Guériguian, J.L., Sawyer, M.E., 1973. A specific progesterone-binding component of human breast cyst fluid. J. Biol. Chem. 248, 5736–5741.
Pei, X.-J., Chen, N., Bai, Y., Qiao, J.-W., Li, S., Fan, Y.-L., Liu, T.-X., 2019. BgFas1: A fatty acid synthase gene required for both hydrocarbon and cuticular fatty acid biosynthesis in the German cockroach, Blattella germanica (L.). Insect Biochem. Mol. Biol. 112, 103203.
Peitsch, M.C., Boguski, M.S., 1990. Is apolipoprotein D a mammalian bilin-binding protein? New Biol. 2, 197–206.
Pfaffl, M.W., 2001. A new mathematical model for relative quantification in real-time RT-PCR. Nucleic Acids Res. 29, e45.
Qiao, J.-W., Fan, Y.-L., Bai, T.-T., Wu, B.-J., Pei, X.-J., Wang, D., Liu, T.-X., 2020. Lipophorin receptor regulates the cuticular hydrocarbon accumulation and adult fecundity of the pea aphid Acyrthosiphon pisum. Insect Sci.
Qiu, Y., Tittiger, C., Wicker-Thomas, C., Le Goff, G., Young, S., Wajnberg, E., Fricaux, T., Taquet, N., Blomquist, G.J., Feyereisen, R., 2012. An insect-specific P450 oxidative decarbonylase for cuticular hydrocarbon biosynthesis. Proc. Natl. Acad. Sci. USA 109, 14858–14863.
Rassart, E., Desmarais, F., Najyb, O., Bergeron, K.-F., Mounier, C., 2020. Apolipoprotein D. Gene 756, 144874.
Ruiz, M., Sanchez, D., Canal, I., Acebes, A., Ganfornina, M.D., 2011. Sex-dependent modulation of longevity by two Drosophila homologues of human Apolipoprotein D, GLaz and NLaz. Exp. Gerontol. 46, 579–589.
Ruiz, M., Sanchez, D., Correnti, C., Strong, R.K., Ganfornina, M.D., 2013. Lipid-binding properties of human ApoD and Lazarillo-related lipocalins: functional implications for cell differentiation. FEBS J. 280, 3928–3943.
Ruiz, M., Wicker-Thomas, C., Sanchez, D., Ganfornina, M.D., 2012. Grasshopper Lazarillo, a GPI-anchored Lipocalin, increases Drosophila longevity and stress resistance, and functionally replaces its secreted homolog NLaz. Insect Biochem. Mol. Biol. 42, 776–789.
Sánchez, D., Ganfornina, M.D., Torres-Schumann, S., Speese, S.D., Lora, J.M., Bastiani, M.J., 2000. Characterization of two novel lipocalins expressed in the Drosophila embryonic nervous system. Int. J. Dev. Biol. 44, 349–359.
Sanchez, D., López-Arias, B., Torroja, L., Canal, I., Wang, X., Bastiani, M.J., Ganfornina, M.D., 2006. Loss of glial lazarillo, a homolog of apolipoprotein D, reduces lifespan and stress resistance in Drosophila. Curr. Biol. 16, 680–686.
Sapountzis, P., Duport, G., Balmand, S., Gaget, K., Jaubert-Possamai, S., Febvay, G., Charles, H., Rahbé, Y., Colella, S., Calevro, F., 2014. New insight into the RNA interference response against cathepsin-L gene in the pea aphid, Acyrthosiphon pisum: Molting or gut phenotypes specifically induced by injection or feeding treatments. Insect Biochem. Mol. Biol. 51, 20–32.
Schal, C., Sevala, V., Cardé, R., 1998. Novel and highly specific transport of a volatile sex pheromone by hemolymph lipophorin in moths. Naturwissenschaften 85, 339–342.
Simon, J.-C., Peccoud, J., 2018. Rapid evolution of aphid pests in agricultural environments. Curr. Opin. Insect Sci. 26, 17–24.
Tsukamoto, K., Mani, D.R., Shi, J., Zhang, S., Haagensen, D.E., Otsuka, F., Guan, J., Smith, J.D., Weng, W., Liao, R., Kolodgie, F.D., Virmani, R., Krieger, M., 2013. Identification of apolipoprotein D as a cardioprotective gene using a mouse model of lethal atherosclerotic coronary artery disease. Proc. Natl. Acad. Sci. USA 110, 17023–17028.
Walker, D.W., Muffat, J., Rundel, C., Benzer, S., 2006. Overexpression of a Drosophila homolog of apolipoprotein D leads to increased stress resistance and extended lifespan. Curr. Biol. 16, 674–679.
Wigglesworth, V.B., 1970. Structural lipids in the insect cuticle and the function of the oenocytes. Tissue Cell 2, 155–179.
Ye, C., An, X., Jiang, Y.-D., Ding, B.-Y., Shang, F., Christiaens, O., Taning, C.N.T., Smagghe, G., Niu, J., Wang, J.-J., 2019. Induction of RNAi Core Machinery's Gene Expression by Exogenous dsRNA and the Effects of Pre-exposure to dsRNA on the Gene Silencing Efficiency in the Pea Aphid (Acyrthosiphon pisum). Front. Physiol. 9, 1906.
Yu, X.-D., Liu, Z.-C., Huang, S.-L., Chen, Z.-Q., Sun, Y.-W., Duan, P.-F., Ma, Y.-Z., Xia, L.-Q., 2016. RNAi-mediated plant protection against aphids. Pest Manag. Sci. 72, 1090–1098.
Zeng, C., Spielman, A.I., Vowels, B.R., Leyden, J.J., Biemann, K., Preti, G., 1996. A human axillary odorant is carried by apolipoprotein D. Proc. Natl. Acad. Sci. USA 93, 6626–6630.
Zhou, Y., Li, Y., Li, X., Li, R., Xu, Y., Shi, L., Wang, H., 2020. Apolipoprotein D in Lepidoptera: Evolution and functional divergence. Biochem. Biophys. Res. Commun. 526, 472–478.
Zhou, Y., Wang, L., Li, R., Liu, M., Li, X., Su, H., Xu, Y., Wang, H., 2018. Secreted glycoprotein BmApoD1 plays a critical role in anti-oxidation and anti-apoptosis in Bombyx mori. Biochem. Biophys. Res. Commun. 495, 839–845.